

# **Dynamical T-matrix theory for high-density excitons in coupled quantum wells**

R. Zimmermann

*Institut für Physik der Humboldt-Universität zu Berlin,*

*Newtonstr. 15, D-12489 Berlin, Germany*

## **Abstract**

Excitons in coupled quantum wells open the possibility to reach high densities close to equilibrium. In a recent experiment employing a lateral trap potential, a blue shift and a broadening of the exciton emission line has been seen [1]. The standard Hartree-Fock treatment can explain the blue shift but fails to give a finite broadening. Starting from the (spin-dependent) many-exciton Hamiltonian with direct and exchange potential, we present a dynamical T-matrix calculation for the single-exciton Green's function which is directly related to the frequency- and angle-resolved photoluminescence. The calculated spectrum is blue shifted and broadened due to exciton-exciton scattering. At high excitation, both the spectrum and the angular emission are getting narrow. This is a direct manifestation for off-diagonal long range order and a precursor of condensation.

## I. INTRODUCTION

On the search for exciton systems where high densities at low temperatures can be reached, coupled quantum wells (CQW) came into the focus recently [2, 3]. Being spatially indirect, the excitons have microsecond lifetimes, and equilibration at Helium temperatures can be expected. In addition, lateral confinement into a stress-induced trap will enforce high local densities. Standard estimates of critical temperatures/critical densities for Bose-Einstein condensation (BEC) gave promising values, thanks to the small exciton mass. However, excitons in CQW feel a strong dipole-dipole repulsion, and expressions valid for a nearly ideal Bose gas cannot be applied. Recent experiments by Snoke and coworkers [1] have shown a substantial blue shift (5 meV) of the exciton emission line under high excitation in a trap, but accompanied by a sizable broadening of the exciton line. For an overview on attempts to find exciton BEC in semiconductors, see the special issue on "Spontaneous Coherence in Excitonic Systems" [4].

A Hartree-Fock treatment of the many-exciton problem can easily explain the blue shift. However, while the Hartree-Fock approach (including a c-number term) is at the heart of the Bogolubov theory of BEC [5], it is not able in principle to describe line broadenings. In order to go one step further, we present here a dynamical T-matrix theory where multiple exciton-exciton (XX) scattering is included, and which gives realistic line shapes. The theory presented is not applicable to the BEC state itself. However, the approach to condensation is investigated in more detail than before. Finding characteristic features in the emission spectrum and its angular dependence [6] may help to specify conditions in favor of BEC.

## II. EXCITONS IN COUPLED QUANTUM WELLS

Applying a static electric field in the growth (z-) direction allows to tune the coupled quantum well such that the indirect exciton state becomes the lowest one (see Fig. 1). The single-exciton wave function can be factorized, denoting the in-plane relative coordinate with  $\mathbf{r}$  and the center-of-mass one with  $\mathbf{R}$ , as

$$\Psi(\mathbf{r}_e, \mathbf{r}_h) = u_e(z_e) u_h(z_h) \phi(\mathbf{r}) \psi(\mathbf{R}). \quad (1)$$

The confinement functions  $u_a(z_a)$  for the CQW system under study are shown in Fig. 1, too. The Schrödinger equation for the 1s exciton wave function  $\phi(\mathbf{r})$  is solved numerically [7] with the

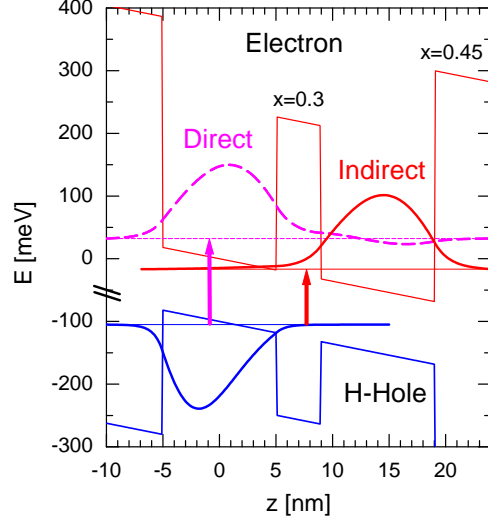


FIG. 1: Band edge diagram for the coupled quantum well system used in Ref. [1]: Two GaAs quantum wells of 10 nm width are separated by an  $\text{Al}_x\text{Ga}_{1-x}\text{As}$  barrier of 4 nm. A static electric field of  $F = 36 \text{ kV/cm}$  is tilting the band edges. Each confinement wave function is plotted with a vertical offset being its energy.

potential

$$v_{eh}(\mathbf{r}) = \int dz dz' \frac{e^2}{4\pi\epsilon_0\epsilon_s\sqrt{r^2 + (z - z')^2}} u_e^2(z) u_h^2(z') \quad (2)$$

and gives an indirect (direct) exciton binding energy of 3.5 (19.1) meV. The calculated radiative lifetimes are  $\tau_{dir} = 31 \text{ ps}$  and  $\tau_{ind} = 0.45 \mu\text{s}$ . Therefore, equilibration of the indirect excitons at low bath temperatures may be achieved.

However, at the same time, indirect excitons feel a strong Coulomb repulsion of dipole-dipole character. Reducing this to a contact potential gives the strength

$$U_d = \int d\mathbf{r} [v_{ee}(\mathbf{r}) + v_{hh}(\mathbf{r}) - 2v_{eh}(\mathbf{r})] . \quad (3)$$

In the strict 2D limit, this would result in the dipole-dipole repulsion of  $U_d = de^2/\epsilon_0\epsilon_s$ , where  $d$  is the effective CQW separation. Additionally, the internal fermionic structure of excitons leads to a (non-local) exchange potential. Bringing this into contact form as well, we have

$$U_x = \sum_{\mathbf{k}, \mathbf{k}'} [2v_{eh}(\mathbf{k} - \mathbf{k}') \phi_{\mathbf{k}}^3 \phi_{\mathbf{k}'} - (v_{ee}(\mathbf{k} - \mathbf{k}') + v_{hh}(\mathbf{k} - \mathbf{k}')) \phi_{\mathbf{k}}^2 \phi_{\mathbf{k}'}^2] . \quad (4)$$

For the CQW of Fig. 1 we have calculated  $U_d = 18.8 \text{ eV nm}^2$  and  $U_x = -8.9 \text{ eV nm}^2$ .

With these ingredients, and taking into account the spin structure of excitons composed from spin 1/2 conduction electrons and spin 3/2 heavy hole states, the following many-exciton boson

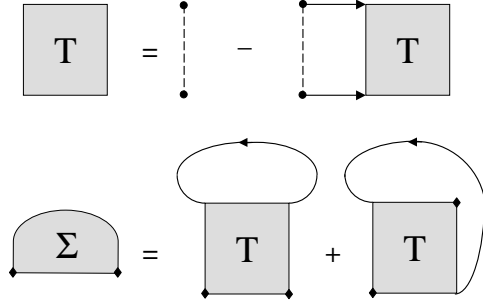


FIG. 2: Diagrammatic representation of the dynamical T-matrix scheme. The full line with arrow denotes the single exciton Green's function  $G_{\mathbf{k}}(z)$ , and the dashed line is the XX interaction  $U^{\pm}$  (for simplicity, we have not resolved the spin degree of freedom here). The two terms in the self energy are the direct and (boson) exchange contributions. For the contact interaction used, they can be combined into one term.

Hamiltonian can be constructed [8]

$$\begin{aligned}
H = & \int d\mathbf{R} \sum_s \Psi_s^\dagger(\mathbf{R}) \left[ -\frac{\hbar^2 \nabla^2}{2M} + V(\mathbf{R}) \right] \Psi_s(\mathbf{R}) + \\
& + \frac{1}{2}(U_d + U_x) \int d\mathbf{R} \sum_{ss'} \Psi_s^\dagger(\mathbf{R}) \Psi_{s'}^\dagger(\mathbf{R}) \Psi_{s'}(\mathbf{R}) \Psi_s(\mathbf{R}) \\
& + U_x \int d\mathbf{R} \sum_{ss'} \left( \frac{1}{4} - \delta_{ss'} \right) \Psi_s^\dagger(\mathbf{R}) \Psi_{-s}^\dagger(\mathbf{R}) \Psi_{-s'}(\mathbf{R}) \Psi_{s'}(\mathbf{R}).
\end{aligned} \tag{5}$$

The spin label  $s$  denotes the four exciton states, which are  $s = \pm 1$  (bright) and  $s = \pm 2$  (dark). The one-exciton potential  $V(\mathbf{R})$  can model a lateral trap confinement, but is not considered here.

### III. DYNAMICAL T-MATRIX THEORY

In diagram language, we sum up multiple XX scattering events to form the dynamical T-matrix  $T_{\mathbf{q}}(z)$ . Plugging this into the one-exciton self energy  $\Sigma_{\mathbf{k}}(z)$  leads to an improved one-exciton propagator  $G_{\mathbf{k}}(z)$ , as depicted in Fig. 2. This selfconsistency cycle has to be repeated up to convergence. The specific spin structure of Eq. (5) allows to split the T-matrix into a bonding/antibonding part  $T^{\pm}$ , which obey

$$T_{\mathbf{q}}^{\pm}(\Omega) = \frac{U^{\pm}}{1 + U^{\pm} \mathcal{G}_{\mathbf{q}}(\Omega)}, \quad U^{\pm} = U_d \pm U_x. \tag{6}$$

The exciton pair propagator (two parallel arrows in Fig. 2) is given by

$$\mathcal{G}_{\mathbf{q}}(\Omega) = \sum_{\mathbf{k}} \int \frac{d\omega}{\pi} \frac{d\omega'}{\pi} A_{\mathbf{k}}(\omega) A_{\mathbf{k}-\mathbf{q}}(\omega') \frac{1 + 2g_B(\hbar\omega - \mu)}{\omega + \omega' - \Omega}, \quad g_B(E) = \frac{1}{\exp(E/k_B T) - 1}. \tag{7}$$

In writing Eq. (7) we have used a fixed chemical potential  $\mu$  in the Bose distribution function  $g_B(\hbar\omega - \mu)$ , independent on spin label. Thus, complete spin relaxation of excitons into equilibrium has been assumed. Taken as it stands, the real part of Eq. (7) has a logarithmic divergency coming from the integration over  $\mathbf{k}$ . This is a well-known shortcoming of using in two dimensions a contact potential. As a remedy, we have chosen to cut off the integration at  $\epsilon_{\mathbf{k}} = 100$  meV, well above any relevant energy scale.

The self energy follows with  $T \equiv (9/2)T^+ + (1/2)T^-$  as

$$\begin{aligned} \Sigma_{\mathbf{k}}(z) = & \sum_{\mathbf{q}} \int \frac{d\omega}{\pi} A_{\mathbf{k}-\mathbf{q}}(\omega) \times \\ & \times \left[ T_{\mathbf{q}}(z + \omega) g_B(\hbar\omega - \mu) + \int \frac{d\omega'}{\pi} \frac{\text{Im}T_{\mathbf{q}}(\omega' - i0) g_B(\hbar\omega' - 2\mu)}{\omega' - z - \omega} \right] \end{aligned} \quad (8)$$

and enters the exciton Green's function resp. its spectral function

$$A_{\mathbf{k}}(\omega) = \text{Im}G_{\mathbf{k}}(\omega - i0) = \frac{\text{Im}\Sigma_{\mathbf{k}}(\omega - i0)}{(\omega - \epsilon_{\mathbf{k}} - \text{Re}\Sigma_{\mathbf{k}}(\omega - i0))^2 + (\text{Im}\Sigma_{\mathbf{k}}(\omega - i0))^2}. \quad (9)$$

For the exciton system, the spectrally and directionally resolved spontaneous optical emission is given by

$$I(\mathbf{k}, \omega) = \mu_{cv} \int d\mathbf{R} d\mathbf{R}' e^{i\mathbf{k}(\mathbf{R}-\mathbf{R}')} \int dt e^{i\omega t} \langle \Psi_s^\dagger(\mathbf{R}, t) \Psi_s(\mathbf{R}', 0) \rangle, \quad (s = \pm 1) \quad (10)$$

which shows clearly the importance of contributions  $\mathbf{R} \neq \mathbf{R}'$  (off-diagonal long range order) for the directional characteristic (dependence on  $\mathbf{k}$ ). Further, Eq. (10) can be simply expressed via the single-exciton propagator resp. the spectral function,

$$I(\mathbf{k}, \omega) \propto i G_{\mathbf{k}}^<(\omega) \equiv g_B(\hbar\omega - \mu) A_{\mathbf{k}}(\omega). \quad (11)$$

For understanding the spectral shape, it is important to note that the spectral function changes sign at the chemical potential  $\mu$  where the Bose distribution function  $g_B(\hbar\omega - \mu)$  has a pole, resulting in a strictly positive emission. Portions below  $\mu$  are due to photon emission accompanied by XX scattering. The classical argument for BEC onset ( $\mu$  is touching the energy of the lowest state) has to be refined here: A phase transition happens if the chemical potential hits the quasiparticle dispersion,  $\text{Re}\Sigma_0(\hbar\omega = \mu) = \mu$ . Then, both the spectrum and the directional characteristic evolve into sharp delta peaks. In Fig. 3, results of the full dynamical T-matrix calculation (at zero momentum) are shown. The exciton emission increases with rising density. The initial increase in line width due to XX scattering turns into sharpening of the spectral line shape (left), while a peak

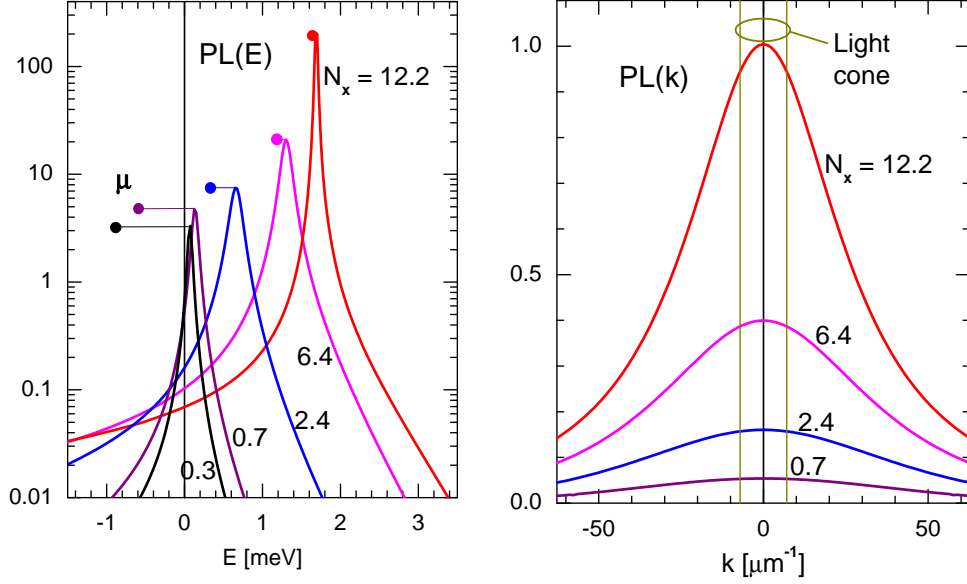


FIG. 3: Emission line shapes in dependence on frequency (left) and on direction (right). The lines are getting sharper as the chemical potential  $\mu$  (dots) approaches the emission maximum (quasiparticle position). The temperature is held fixed at  $T = 5$  K, and exciton densities  $N_X$  are given in units of  $10^{10} \text{ cm}^{-2}$ . The light cone (marked by vertical lines on the right) sets a limit for the observability of the angular emission.

in the angle resolved emission (right) evolves. However, condensation is not achieved at  $T = 5$  K for the density range considered.

The exciton densities given in Fig. 3 are calculated with the standard expression using the momentum- and frequency-dependent spectral function Eq. (9) and the Bose distribution function. It is worth noting that the T-matrix comes out appreciably smaller than the bare interaction ( $U^\pm$ ). Consequently, at a given density, the blue shift of the emission is much less than a simple Hartree-Fock argument would predict. Obviously, the strong dipole-dipole repulsion and its dynamical character hinder an easy build-up of coherence. Further calculations including the confining action of a lateral trap shall specify more precisely conditions for condensation in coupled quantum wells.

- 
- [1] D.W. Snoke, Y. Liu, Z. Vörös, L. Pfeiffer, and K. West, *Solid State Comm.* **134**, 37 (2005).
  - [2] L.V. Butov, *Nature* **417**, 47 (2002); *Solid State Comm.* **127**, 89 (2003).
  - [3] D. Snoke, S. Deney, Y. Liu, L. Pfeiffer, and K. West, *Nature* **418**, 754 (2002).
  - [4] Special issue, *Solid State Comm.* **134**, p. 1–164 (2005).

- [5] A. Griffin, Phys. Rev. B **53**, 9341 (1996).
- [6] J. Keeling, L.S. Levitov, and P.B. Littlewood, Phys. Rev. Letters **92**, 176402 (2004).
- [7] R. Zimmermann, Solid State Comm. **134**, 43 (2005).
- [8] S. Ben-Tabou de-Leon and B. Laikhtman, Phys. Rev. B **63**, 125306 (2001).